Environmental Earth Sciences (2019) 78:21
https://doi.org/10.1007/s12665-018-8011-4

THEMATIC ISSUE

Modelling tool to assess membrane regeneration by periodical hydraulic cleaning and fouling control in pressurized membrane process for surface water treatment

Amine Charfi[1] · Hoseok Jang[1] · Jeonghwan Kim[1]

Received: 22 April 2018 / Accepted: 18 December 2018 / Published online: 2 January 2019

Abstract

In this study, a mathematical model was developed to assess fouling as well as membrane regeneration in a pressurized, hollow-fiber membrane system for the treatment of highly turbid surface water using periodical cleaning by backwashing and forward flushing. The model was validated using experimental data of trans-membrane pressure obtained when filtering separately, a SiO_2 solution, a mixed SiO_2/sodium alginate (SA) solution, a mixed SiO_2/bovin serum albumin (BSA) solution and a mixed SiO_2/humic acid (HA). Experimental and theoretical studies highlighted the synergistic fouling effect between SiO_2 simulating the colloidal particles and the different elements (HA, SA and BSA) simulating the natural organic matter. Protein fouling was mitigated when mixed with SiO_2. While the highest fouling rate was obtained for mixed SiO_2/SA solution, the majority of this fouling was removed by periodic cleaning. Moreover, mixed SiO_2/HA solution showed also high fouling which was mainly irreversible.

Abbreviations

C	Total foulants' concentration (kg m^{-3})
J	Permeate flux (m^3 m^{-2} s^{-1})
k	Specific cake resistance kinetic coefficient (–)
k_1	Specific cake resistance decrease coefficient (–)
k_2	Coefficient of the parameter σ decrease (–)
m_a	Specific matter mass attached to membrane (kg m^{-2})
m_c	Specific cake mass (kg m^{-2})
m_d	Specific matter mass detached from membrane (kg m^{-2})
R_0	Membrane intrinsic resistance (m^{-1})
R_c	Cake resistance (m^{-1})
TMP	Trans-membrane pressure (Pa)
α	Specific cake resistance (m kg^{-1})
α_0	Initial specific cake resistance (m kg^{-1})
γ	Back-diffusion coefficient (m^2 kg^{-1})
μ	Permeate viscosity (Pa s)
σ	Specific cake mass decrease parameter (–)

This article is a part of Topical Collection in Environmental Earth Sciences on Water Sustainability: A Spectrum of Innovative Technology and Remediation Methods, edited by Dr. Derek Kim, Dr. Kwang-Ho Choo, and Dr. Jeonghwan Kim.

✉ Jeonghwan Kim
jeonghwankim@inha.ac.kr

[1] Department of Environmental Engineering, Inha University, 100 Inharo, Namgu, Incheon, Republic of Korea

Introduction

Low-pressure driven membrane filtration processes such as microfiltration and ultrafiltration have been widely considered for surface water treatment since they are able to totally remove pathogens, colloidal matter and turbidity to meet stringent water quality standards. Nevertheless, membrane fouling is still the main issue which hinders the function of membrane filtration. Membrane fouling occurs when rejected components are deposited on the membrane surface or trapped within the membrane pores leading to lower membrane productivity, higher energy consumption and shorter life-time. Physical cleaning methods such as forward flushing, backwashing, vibration, air flushing, back-pulsing and air scouring are able to eliminate the majority of membrane fouling so-called a reversible fouling (Cho et al. 2017). However, a fraction of membrane permeability cannot be recovered fully due to gradual accumulation of irreversible foulant. This requires chemical cleaning likely to damage the membrane over time (Howe and Clark 2002; Gao et al. 2011).

Numerous parameters could impact on irreversible fouling. The humic substances, protein-like matter, fulvic acid

like materials and colloidal/particulate matter are the major responsible of irreversible fouling in surface water ultrafiltration (Munla et al. 2012; Peiris et al. 2013; Chu et al. 2015; Gamage and Chellam 2014). Moreover, Chu et al. (2015) showed that the inorganic matter such as Fe, Al and Ca contributed also to some extent to the irreversible fouling during the ultrafiltration of raw surface water. Irreversible fouling has been shown to be occurring not only during short-term membrane operations (Kimura et al. 2004; Cho et al. 2000) but also during long-term membrane operations (Chu et al. 2015). Different mechanisms were proven to promote irreversible fouling such as the adsorption of foulants on the membrane and within its pores as well as deposit consolidation (Crozes et al. 1993; Yamamura et al. 2007). Moreover, other parameters impact on irreversible fouling development such as membrane characteristics (Yamamura et al. 2007). Chang et al. (2017) showed that Polyvinyl difluoride (PVDF) membranes characterized by lower cohesive free energy than Polyethersulfone (PES) and Cellulose acetate (CA) membranes would foster irreversible fouling. Furthermore, the backwashing solution characteristics can also develop irreversible fouling, by showing that DI water for backwashing results in lower irreversible fouling compared to using permeate solution (Chang et al. 2017).

Numerous models have been considered to quantify fouling in microfiltration and ultrafiltration when treating surface water (Bérubé and Lei 2006). The models proposed by Hermia (1982) have been widely used to understand membrane fouling (Liu et al. 2016; Charfi et al. 2017a) considering separately different fouling mechanisms such as pore constriction, pore blocking, intermediate blocking and cake formation, while other models combined those mechanisms (Bolton et al. 2006; Charfi et al. 2017b; Hou et al. 2017). Nevertheless, while most of the proposed models assessed fouling in continuous membrane operation, few models considered the effect of periodical cleaning by forward and backwashing on fouling mitigation as well as on the irreversible fouling mechanism (Lin and Bérubé 2007). In this study, a mechanistic model was developed to assess the periodical cleaning effect and its effect on the irreversible fouling when treating highly turbid surface water with a pressurized, hollow-fiber membrane system.

Materials and methods

Experimental set-up

A laboratory-scaled, experimental set-up of pressurized ultrafiltration (UF) membrane was developed as shown in Fig. 1. The membrane module used, consists of 100 polysulfone hollow-fibers. The membrane characteristics are shown in Table 1. A Set-point permeate flux was maintained by micro-gear pump (WT3000-1JA, Longerpump, China). Flow rates and pressures were measured by impeller flow meter (FHK G1/4, Digmesa, Swiss) and digital pressure gauge (PSAN-L1CA, Autonics, Korea), respectively. System control and data registration were realized by PLC installed customized software. The system was operated continuously. The driving force of the filtration process is ensured by the feed pump, which enables the feed solution to flow through the membrane matrix. A flow sensor downstream the membrane detects the permeate flux decrease due to membrane fouling and sends a signal to the feed pump controller to increase pump speed to maintain a constant permeate flux.

Feed solutions

In this study, four synthetic surface water solutions with a turbidity of 10 NTU were prepared using 50 ppm of SiO_2 only to simulate colloidal particles, and by mixing separately SiO_2 solution with 10 ppm of bovin serum albumin (BSA), 10 ppm of sodium alginate (SA) and 10 ppm of humic acid (HA), respectively. The particle size distributions of filtered solutions were analyzed by light scattering method with a particle size analyzer (Malvern Master sizer 2000, UK). Measurement revealed average sizes of 14.53 µm for SiO_2 solution, 12.83 µm for mixed SiO_2/BSA, 15.06 µm for mixed SiO_2/HA and 15.65 µm for mixed SiO_2/SA.

Operational conditions

Dead-end filtration experiments were conducted in outside-in mode at constant permeate flux of 100 L/m^2.hr (LMH). To ensure the dead end filtration mode, the discharge valve was closed during filtration process. Every 30 min of filtration, a periodical physical cleaning of 30 s by backwashing followed by 30 s of forward flushing was applied using the membrane permeate collected. The backwashing was performed in inside–outside mode, inversely to filtration direction. Forward flushing was performed by flowing the permeate solution along the membrane surface to remove foulants deposited on the membrane. Forward flushing flux was equal to the permeate flux applied, while backwashing flux was 2 times higher than the permeate flux. To prevent SiO_2 particles' settling, the feed solution was stirred in the feed tank during experiment. Turbidity of retentate and permeate solutions were measured by turbidity meter (2020we, LaMOTTE, USA).

Model development

The proposed model aims to assess fouling during surface water treatment by a pressurized membrane process when physical cleaning is applied periodically. Two phases are then considered, a filtration phase and a cleaning phase.

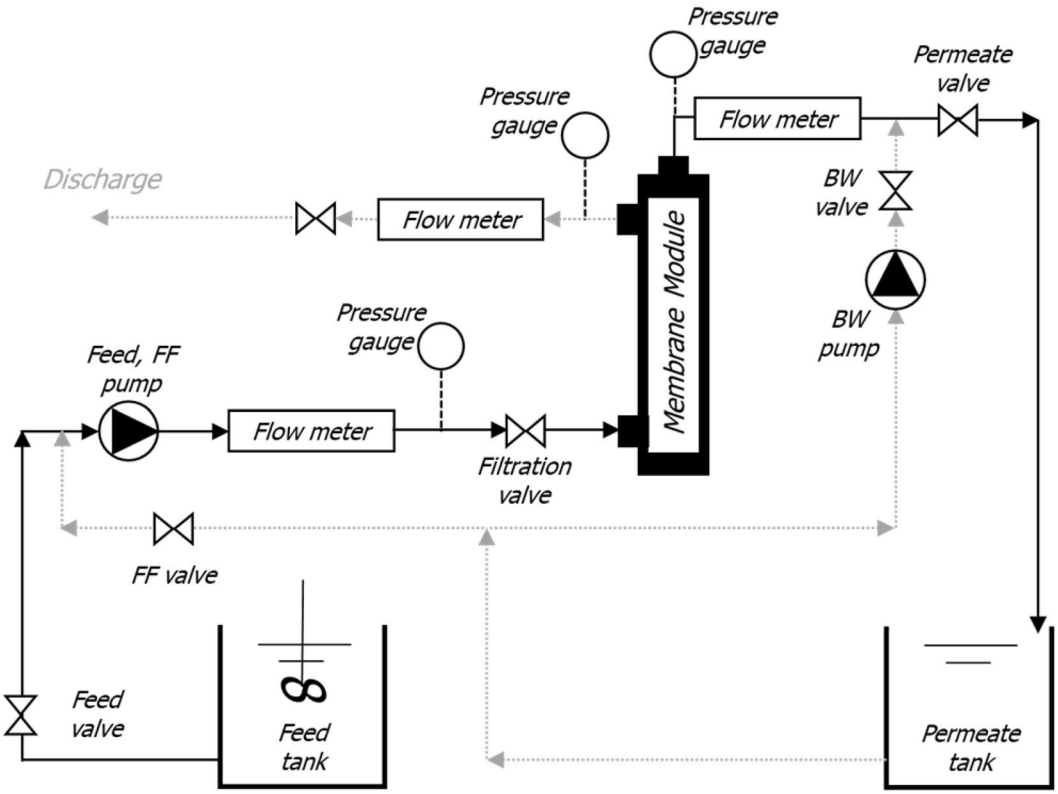

Fig. 1 Experimental set-up of pressurized UF membrane system

Table 1 Membrane specifications

Parameter	Factor	Unit
Material	Polysulfone	
Pore size	0.05	μm
Area	0.11	m^2
Fibers ID/OD	0.9–1.4	mm
Permeability at 28 ± 0.9 °C	594 ± 94	L m^{-2} h^{-1} bar^{-1}

During filtration phase, a dead-end mode was considered at constant permeate flux. To describe fouling, the model simulates the TMP variation with time by a resistance in series model as expressed in Eq. 1.

$$\mathrm{TMP} = J \cdot \mu \cdot \left(R_0 + R_c\right) \tag{1}$$

where J is the permeate flux (m^3 m^{-2} s^{-1}), μ is permeate viscosity (Pa s), R_0 is membrane intrinsic resistance (m^{-1}) and R_c is cake resistance (m^{-1}).

Moreover, the model assumes fouling occurring due to the deposit of foulants on the membrane surface to form a cake layer. The cake resistance is then expressed by Eq. 2.

$$R_c = \alpha \cdot m_c \tag{2}$$

where α is the specific cake resistance (m kg^{-1}) and m_c the specific cake mass (kg m^{-2}).

The specific cake mass accumulated on the membrane surface expressed by Eq. 3, is assumed as the difference between (1) the specific mass of matter dragged by convective forces and attached to the membrane surface, and (2) the specific mass of matter detached by physical cleanings

$$\frac{dm_c}{dt} = \frac{dm_a}{dt} - \frac{dm_d}{dt} \tag{3}$$

The specific mass attached to the membrane is assumed proportional to the permeate flux and total foulants' concentration (Eq. 4)

$$\frac{dm_a}{dt} = J \cdot C \tag{4}$$

where J is the permeate flux (m^3 m^{-2} s^{-1}) and C is the foulants' concentration (kg m^{-3}).

The specific mass detached by physical cleaning is assumed proportional to the specific mass attached and the accumulated specific cake mass (Eq. 5).

$$\frac{dm_d}{dt} = \gamma \cdot \frac{dm_a}{dt} \cdot m_c \tag{5}$$

In this study, the cake was assumed compressible and its specific resistance was then considered increasing exponentially with time according to a first order kinetic equation as shown in (Eq. 6).

$$\frac{d\alpha}{dt} = k \cdot \alpha \tag{6}$$

During the periodical cleaning phase, the specific cake mass decrease was expressed by a first order differential equation (Eq. 7)

$$\frac{dm_c}{dt} = -\sigma \cdot m_c \tag{7}$$

Similarly, the specific cake resistance assumed decreasing during the cleaning phase, is expressed by a first order differential equation (Eq. 8).

$$\frac{d\alpha}{dt} = -k_1 \cdot \alpha \tag{8}$$

The model takes into account the irreversible fouling mechanism usually highlighted in surface water treatment by membrane processes. This phenomenon was introduced in the proposed model during cleaning phase, by assuming the decrease of the kinetic constant σ of the specific cake mass variation (Eq. 9). The parameter σ in this study expresses the efficiency of the periodical cleaning to decrease the cake mass and to regenerate the membrane. The development of an irreversible layer would lead to a decrease of the periodical cleaning efficiency and consequently decreases the parameter σ.

$$\frac{d\sigma}{dt} = -k_2 \cdot \sigma \tag{9}$$

Model validation method

To validate the model, it was compared to the experimental data of normalized pressure registered on the pressurized membrane system. The model fitting with experimental data as well as the model parameters' identification were realized by the least squares method, using MatLab software. This method is based on optimizing the model parameters permitting the minimization of the least squares (LS) function as shown in Eq. 10.

$$LS = \frac{1}{TMP_0} \sum \left(TMP_{experimental} - TMP_{simulation}\right)^2 \tag{10}$$

Regarding the possible existence of different parameters sets leading to the same fitting quality, we refers to as "parameter identifiability". The theoretical identifiability study is usually difficult to realize. It is why a numerical approach has been rather used which consists in running a large number of optimizations while varying the initial conditions for the parameters to be identified. The application of this procedure in the present case revealed a unique combination of optimized parameters.

Results and discussion

Experimental results

The effect of the major foulant materials encountered in surface water, namely colloidal particulates, polysaccharides, proteins and humic such as substances, on normalized TMP variation was studied (Fig. 2). As expected, a TMP increase was registered in all studied cases, however, the fouling intensity obtained varied according to the foulant material tested. The particle size distributions of filtered particles were higher than membrane pore size, and thus cake building was likely to be responsible of membrane fouling. The cake deposit was confirmed for all studied cases through Scanning Electron Microscopy (SEM) images obtained after the first 30 min of filtration and shown in Fig. 3. Filtering a mixed solutions of SiO_2/SA or SiO_2/HA led to higher TMP increase than the filtration of SiO_2 only, which highlights the effect of SA and HA on fouling increase as they influence the particulate layer structure (Fig. 3a, b, d). Furthermore, NOM was observed to increase fouling irreversibility by membrane adsorption and gel-layer formation (Wiesner and Chellam 1999; Nghiem et al. 2006). In fact, the NOM are adsorbed on the polymeric membrane material, moreover, NOM bind together to form a cohesive and stable gel layer on the membrane surface as well as in the membrane pores, which is difficult to remove by hydraulic backwashing. Furthermore, the rough surface of the membrane helps the gel layer adhesion

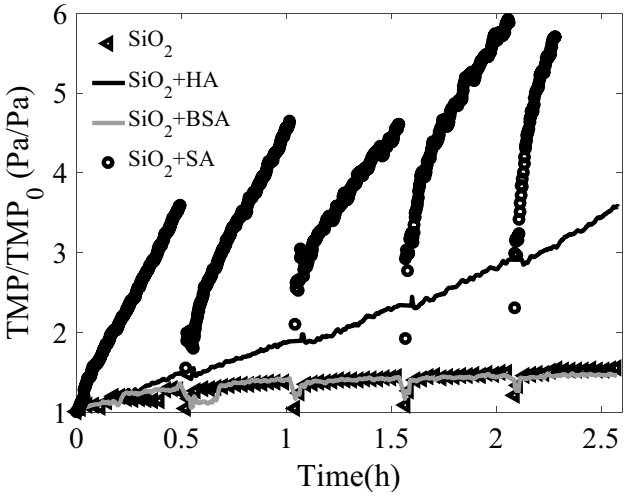

Fig. 2 Comparison of normalized TMP increase with different foulant materials

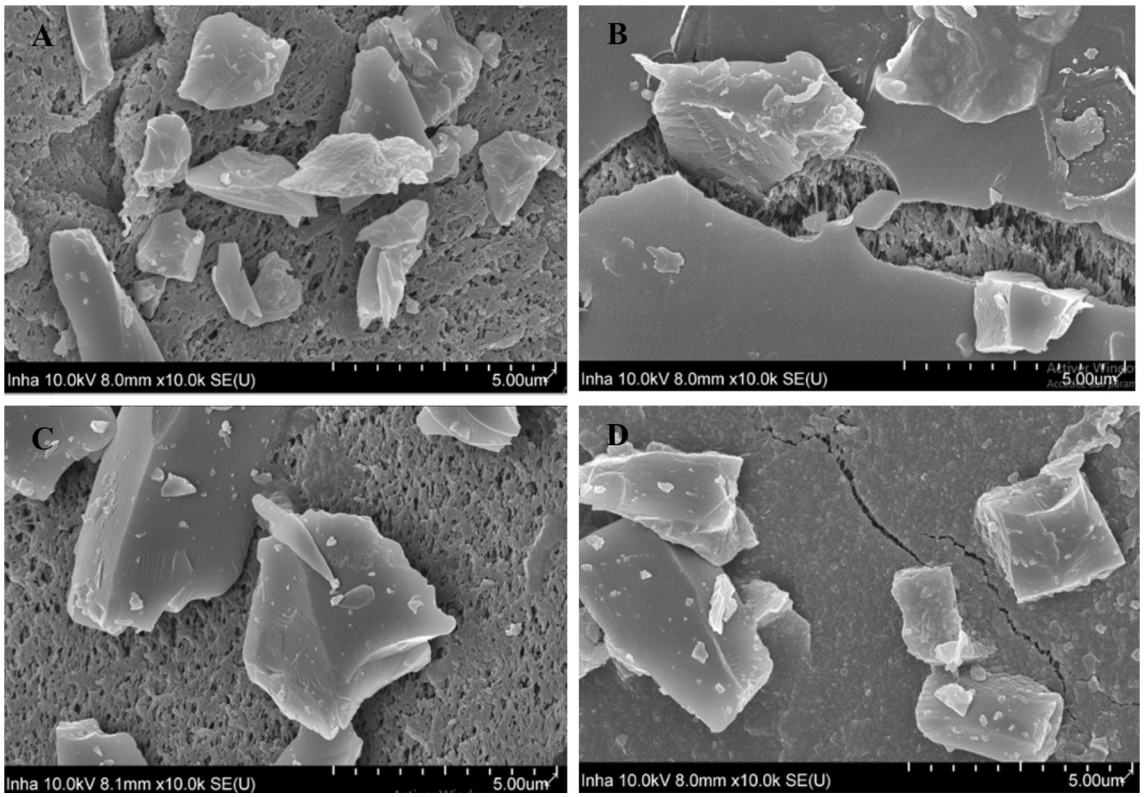

Fig. 3 SEM images obtained after 30 min of filtration of **a** SiO_2 only, **b** mixed SA and SiO_2, **c** mixed BSA and SiO_2 and **d** mixed HA and SiO_2

(Lee et al. 2004). Adding organics to particulate solution results in a fouling cake layer with reduced porosity as compared to individual particle filtration (Jermann et al. 2008).

The highest TMP increase was obtained when filtering a mixed solution of SiO_2/SA. Those results were widely observed in previous works showing the significant effect of polysaccharides on initial pore blocking and cake layer formation (Jermann et al. 2007; Kimura et al. 2004). The alginate retained in the silica fouling layer leads to partial filling of the fouling layer interstices (Fig. 3b). Chen et al. (2006) observed alginate and inorganic particles to form stable colloids. Even if higher TMP was obtained with SA solution, a better membrane recovery was realized which means that most of the fouling developed was reversible. Nonetheless, a fraction of irreversible fouling of 0.39 was also obtained within 2 h of operation. Furthermore, Kimura et al. (2004) showed the irreversible fouling due to the neutral polysaccharide fraction. Little adsorption of alginate on membrane was also observed by Jermann et al. (2007) showing that the irreversible fouling would be due to pore blocking or the silica fouling layer counteracting alginate back-diffusion from the membrane. The presence of alginate can result in increased attachment of silica particle onto the membrane.

Filtering a mixed solution of SiO_2/HA, led to a significant TMP increase, which was lower than the SA case. Moreover, the fouling was found to be mainly irreversible, corresponding to a fraction of 0.98 of the total fouling reached within 2 h of operation. Many previous works found that humic substances were the main foulants responsible of irreversible fouling in surface water filtration (Peiris et al. 2010). Synergistic fouling effect of the various substances during premixed silica and HA filtration was caused by interactions between HA and silica in solution. Significant adsorption of HA on the membrane as well as on the silica particles would be responsible of the development of low porosity fouling layer, highly irreversible (Peiris et al. 2013).

As expected, TMP increase obtained when filtering a solution of SiO_2 only, was lower than the case of SA and HA. While the contribution of colloidal particulate matter in membrane fouling was found mainly effective on reversible fouling rather than irreversible one (Howe and Clark 2002; Peldszus et al. 2011; Peiris et al. 2013), our study revealed a significant rate of irreversible fouling due to silica deposit equal to 0.89 of total fouling occurring within 2 h of operation. Another potential cause of the backwashing efficiency decrease, is the hydraulic variations in backwashing. It is likely that once part of the fouling cake is removed more water passes through this region and is not available to remove other blocked areas.

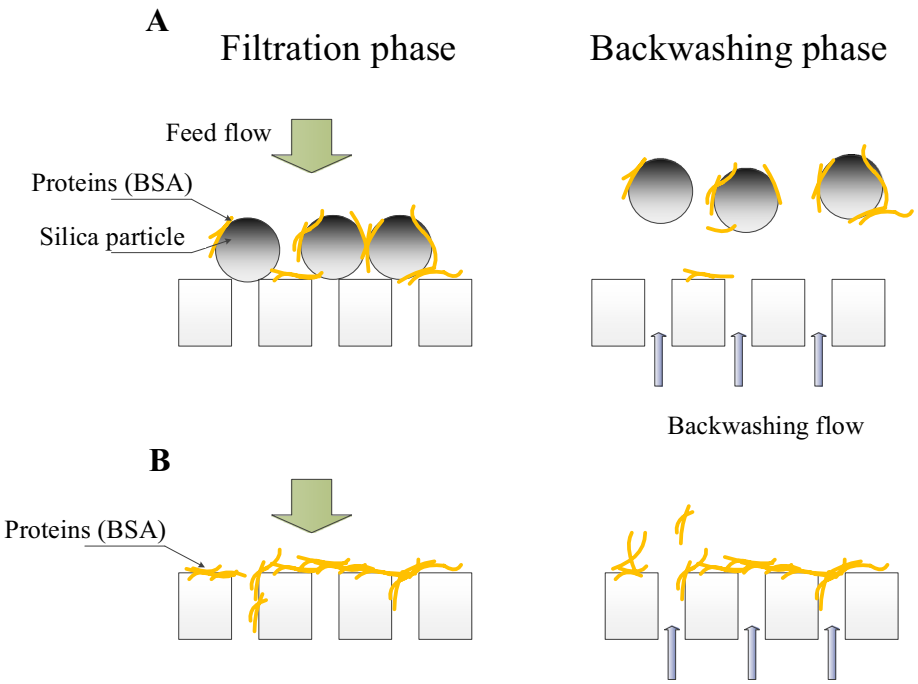

Fig. 4 Conceptual understanding of periodical cleaning efficiency when filtering **a** mixed SiO_2/BSA solution and **b** BSA only

When filtering a mixed solution of SiO_2/BSA, similar TMP trend as in the case of SiO_2 only, was obtained. Similar SEM images were also obtained (Fig. 3a, c) showing mainly a deposit of silica particles. Even if the contribution of proteins was proven to have significant effect on membrane fouling and mainly on the irreversible fouling (Jones and O'Melia 2001; Peldszus et al. 2011), in our study BSA effect on membrane fouling seems not significant. This would be due to the adsorption of proteins on silica particles instead of being adsorbed on the membrane surface which would mitigate their effect on membrane fouling as it is shown in Fig. 4 which displays the difference of the periodical cleaning by backwashing when filtering a mixed SiO_2/BSA solution (Fig. 4a) and a solution of BSA only (Fig. 4b). BSA adsorption on silica particles are not clear on the SEM image shown in Fig. 3c. However, since it displays only a small fraction of the membrane, this image could be non-representative of the mechanisms occurring throughout the membrane surface.

Table 2 Model parameters considered for model simulations

Parameters	Meaning	Values
J	Permeate flux (LMH)	100
μ	Permeate viscosity (Pa s)	10^{-3}
C	Total foulants concentration (g L^{-1})	60×10^{-3}
R_0	Intrinsic membrane resistance (m^{-1})	5×10^{11}

Table 3 Model parameters' values identified by least squares method

Parameters	SiO_2	SiO_2/SA	SiO_2/BSA	SiO_2/HA
α_0	2.10×10^{11}	10×10^{11}	2.16×10^{11}	0.4×10^{11}
k	7×10^{-5}	15×10^{-3}	7×10^{-5}	2.5×10^{-5}
γ	7×10^{-3}	4.3×10^{-3}	7×10^{-3}	1×10^{-6}
σ	2×10^{-2}	2×10^{-2}	2×10^{-2}	0.3×10^{-2}
k_1	1×10^{-4}	4×10^{-4}	4×10^{-4}	0.1×10^{-4}
k_2	1.8×10^{-3}	1.5×10^{-3}	1.5×10^{-3}	5×10^{-3}

Model comparison with experimental data

To validate the developed model it was compared with experimental data obtained when filtering solutions of SiO_2 only, mixed SiO_2/SA, mixed SiO_2/BSA and mixed SiO_2/HA. The model parameters determined experimentally are shown in Table 2. Six model parameters were identified using least squares method (Table 3). Three parameters are related to the filtration phase, namely the initial specific cake resistance α_0, the specific cake resistance kinetic coefficient k relative to the cake compression with filtration time and the back-diffusion coefficient γ. Three other parameters are related to the periodical cleaning phase, namely the specific cake mass decrease parameter, σ, the specific cake resistance decrease coefficient, k_1, the coefficient of the parameter σ decrease, k_2.

The comparison of model simulations and experimental data (Fig. 5) shows satisfactory fitting. The model approach developed was effective to simulate normalized TMP increase for different studied cases. Nonetheless, the slight discrepancy observed would be due to the limited hypothesis assumed in the model. In fact other

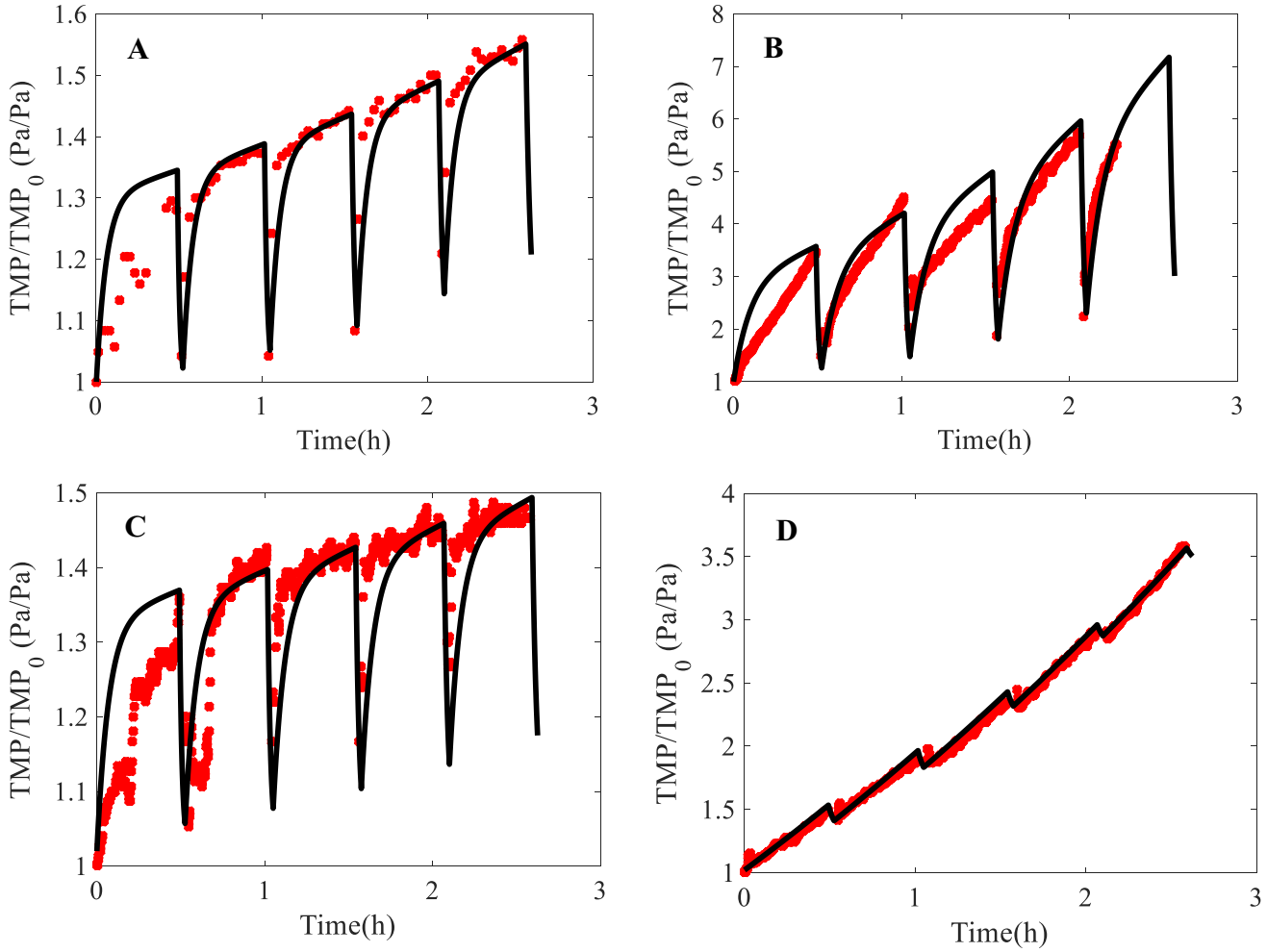

Fig. 5 Comparison of model and experimental data obtained when filtering solutions of **a** SiO_2 only, **b** mixed SA and SiO_2, **c** mixed BSA and SiO_2 and **d** mixed HA and SiO_2

mechanisms could affect the TMP increase such as the pore blocking mechanism.

The initial specific cake resistance α_0 values identified, show the highest value for mixed SiO_2/SA solution of 10×10^{11} m kg^{-1}, the high stickiness of SA and its synergistic fouling effect when combined with SiO_2 would be behind the high initial specific cake resistance as well as the highest value of the parameter k relative to the cake compressibility. On the contrary, the lowest α_0 value and the lowest k parameter value equal to 0.4×10^{11} m kg^{-1} and 2.5×10^{-5}, respectively, were obtained for mixed SiO_2/HA solution. Those low values would be relative to a high cake porosity. The negatively charged HA adsorbed on the deposited silica particles would lead, by repulsive effect, to higher cake porosity. In the other hand the lowest back-diffusion coefficient γ of 1×10^{-6} m^2 kg^{-1} was obtained for SiO_2/HA solution. The high adsorption of HA on the membrane would explain its low back-diffusion. The specific cake mass decrease parameter, σ value is relative to the cleaning efficiency to decrease cake mass. The highest back-diffusion coefficient of 7×10^{-3} m^2 kg^{-1} was obtained for SiO_2 solution and mixed SiO_2/BSA solution, which shows lower adsorption of foulants. Even if protein-like substances were proven to be highly adsorbed on polymeric membrane (Peldszus et al. 2011), low adsorption was found in our study. The adsorption of BSA on silica particles would hinder BSA adsorption on membrane (Fig. 4). Similar σ values were obtained for all studied cases, except for SiO_2/HA solution showing lower value of 0.3×10^{-2} which means lower cleaning efficiency and consequently higher irreversible fouling. HA has been widely proven to be responsible of irreversible fouling (Peiris et al. 2013). This effect is further highlighted through the parameter k_2 values. A positive value of k_2 means that the cleaning efficiency keeps decreasing with time due to an increasing irreversible fouling. An irreversible fouling seems then occurring in all studied cases. The highest value of the parameter k_2 obtained for SiO_2/HA, shows that the irreversible fouling is more significant in this case. The

parameter k_1 is related to the cleaning efficiency to decrease the specific cake resistance. High k_1 value of 4×10^{-4} was obtained for SiO_2/SA and SiO_2/BSA, shows that the cake developed in those cases was more reversible. The lowest k_1 value obtained for SiO_2/HA, is in line with the previous results showing higher irreversible fouling for this case.

Conclusions

A mathematical model was developed to simulate fouling in a pressurized membrane system treating high turbidity surface water when applying periodical cleaning using permeate solution. The model allows to assess the efficiency of periodical cleaning on fouling control and consequently the irreversible fouling effect. Both experimental and theoretical study showed the synergistic fouling effect of SiO_2 and SA leading to the highest and more reversible fouling compared with HA and BSA. The synergistic effect of SiO_2 and HA led to a high and mainly irreversible fouling.

Acknowledgements This research was a part of the project titled 'Manpower training program for ocean energy', funded by the Ministry of Oceans and Fisheries, Korea. This work was supported by the Korea Research Fellowship Program through the National Research Foundation (NRF) funded by the Ministry of Science and ICT (NRF-2015H1D3A1059895).

References

Bérubé PR, Lei E (2006) The effect of hydrodynamic conditions and system configurations on the permeate flux in submerged hollow fiber membrane system. J Memb Sci 271:29–37

Bolton GR, Boesch AW, Lazzara MJ (2006) The effects of flow rate on membrane capacity: development and application of adsorptive membrane fouling models. J Memb Sci 279:625–634

Chang H, Liu B, Liang H, Yu H, Shao S, Li G (2017) Effect of filtration mode and backwash water on hydraulically irreversible fouling of ultrafiltration membrane. Chemosphere 179:254–264

Charfi A, Jang H, Kim J (2017a) Membrane fouling by sodium alginate in high salinity conditions to simulate biofouling during seawater desalination. Biores Technol 240:106–114

Charfi A, Aslam M, Lesage G, Heran M, Kim J (2017b) Macroscopic approach to develop fouling model under GAC fluidization in anaerobic fluidized bed membrane bioreactor. J Ind Eng Chem 49:219–229

Chen KL, Mylon SE, Elimelech M (2006) Aggregation kinetics of alginate coated hematite nanoparticles in monovalent and divalent electrolytes. Environ Sci Technol 40:1516–1523

Cho J, Amy G, Pellegrino J (2000) Membrane filtration of natural organic matter: factors and mechanisms affecting rejection and flux decline with charged ultrafiltration (UF) membrane. J Memb Sci 164:89–110

Cho Y, Kim D, Kim J, Jang M, Wachinski AM (2017) Scale-up testing of a novel cleaning method for low-pressure hollow fiber membranes treating high algae surface waters. Environ Eng Sci 34(11):835–843

Chu KH, Yoo SS, Yoon Y, Ko KB (2015) Specific investigation of irreversible membrane fouling in excess of critical flux for irreversibility: a pilot-scale operation for water treatment. Sep Purif Technol 151:147–154

Crozes G, Anselme C, Mallevialle J (1993) Effect of adsorption of organic matter on fouling of ultrafiltration membranes. J Membr Sci 84:61–77

Gamage NP, Chellam S (2014) Mechanisms of physically irreversible fouling during surface water microfiltration and mitigation by aluminium electroflotation pretreatment. Environ Sci Technol 48:1148–1157

Gao W, Liang H, Ma J, Han M, Chen ZL, Han ZS, Li GB (2011) Membrane fouling control in ultrafiltration technology for drinking water production: a review. Desalination 272:1–8

Hermia J (1982) Constant pressure blocking filtration laws-application to power law non-newtonian fluids. Trans Inst Chem Eng 60:183–187

Hou L, Gao K, Li P, Zhang X, Wang Z, Song P, Yao W (2017) A kinetic model for calculating total membrane fouling resistance in chemical cleaning process. Chem Eng Res Des 128:59–72

Howe KJ, Clark MM (2002) Fouling of microfiltration and ultrafiltration membranes by natural waters. Environ Sci Technol 36:3571–3576

Jermann D, Pronk W, Meylan S, Boller M (2007) Interplay of different NOM fouling mechanisms during ultrafiltration for drinking water production. Water Res 41:1713–1722

Jermann D, Pronk W, Kagi R, Halbeisen M, Boller M (2008) Influence of interactions between NOM and particles on UF fouling mechanisms. Water Res 42:3870–3878

Jones KL, O'Melia CR (2001) Ultrafiltration of protein and humic substances: effect of solution chemistry on fouling and flux decline. J Memb Sci 193:163–173

Kimura K, Hane Y, Watanabe Y, Amy G, Ohkuma N (2004) Irreversible membrane fouling during ultrafiltration of surface water. Water Res 38:3431–3441

Lee N, Amy G, Croué JP, Buisson H (2004) Identification and understanding of fouling in low pressure membrane (MF/UF) filtration by natural organic matter (NOM). Water Res 38:4511–4523

Lin H, Bérubé PR (2007) Modeling the impact of permeate flux and hydrodynamic conditions on fouling in submerged hollow fiber membranes. Water Sci Technol Water Supp 7(4):111–118

Liu J, Dong B, Cao B, Zhao D, Wang Z (2016) Microfiltration process for surface water treatment irreversible fouling identification and chemical cleaning. RSC Adv 6:114005–114013

Munla L, Peldszus S, Huck PM (2012) Reversible and irreversible fouling of ultrafiltration ceramic membranes by model solutions. J Am Water Works Ass 104(10):E540–E554

Nghiem LD, Oschmann N, Schafer AI (2006) Fouling in greywater recycling by direct ultrafiltration. Desalination 187:283–290

Peiris RH, Budman H, Moresoli C, Legge RL (2010) Understanding fouling behavior of ultrafiltration membrane processes and natural water using principal component analysis of fluorescence excitation-emission matrices. J Memb Sci 357:62–72

Peiris RH, Jaklewicz M, Budman H, Legge RL, Moresoli C (2013) Assessing the role of feed water constituents in irreversible membrane fouling of pilot-scale ultrafiltration drinking water treatment systems. Water Res 47:3364–3374

Peldszus S, Hallé C, Peiris RH, Hamouda M, Jin X, Legge RL, Budman H, Moresoli C, Huck PM (2011) Reversible and irreversible low-pressure membrane foulants in drinking water treatment: identification by principal component analysis of fluorescence EEM and mitigation by biofiltration pretreatment. Water Res 45:5161–5170

Wiesner MR, Chellam S (1999) Peer reviewed: the promise of membrane technology. Environ Sci Technol 33:360A–366A
Yamamura H, Kimura K, Watanabe Y (2007) Mechanism involved in the evolution of physically irreversible fouling in microfiltration and ultrafiltration membranes used for drinking water treatment. Environ Sci Technol 41:6789–6794